

The local field experiment is fully applicable to other spin-pairs, including (but not limited to) $^{13}\text{C}-^1\text{H}$, $^{31}\text{P}-^1\text{H}$, and $^{13}\text{C}-^{15}\text{N}$.

Acknowledgment. This research was supported by the National Institutes of Health (GM-23403, GM-23289, GM-23316, and

RR-00995) and by the National Science Foundation through its support of the Francis Bitter National Magnet Laboratory (DMR-8211416). J.E.R. was the recipient of an NIH Postdoctoral Fellowship (GM-09108). We thank T. F. Koetzle for communicating to us the crystallographic data on tryptophan.

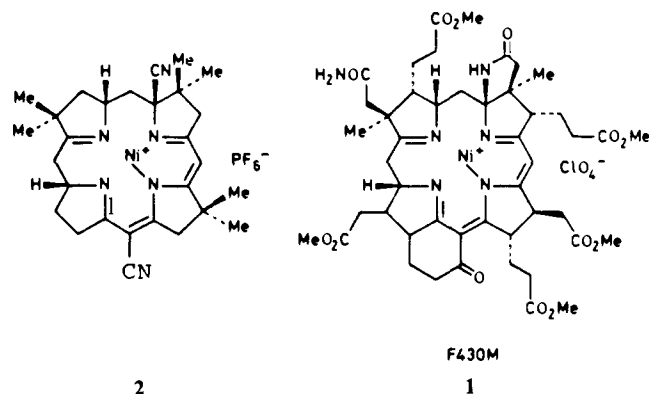
Axial Ligation-Induced Structural Changes in Nickel Hydrocorphinoids Related to Coenzyme F₄₃₀ Detected by Raman Difference Spectroscopy[†]

J. A. Shelnutt

Contribution from the Process Research Division 6254, Sandia National Laboratories, Albuquerque, New Mexico 87185. Received November 14, 1986

Abstract: Raman difference spectroscopy provides a structural probe of the state of axial ligation of Ni(II) in nickel corphinoids of the type occurring in coenzyme F₄₃₀ of the methylreductase enzyme of methanogenic bacteria. The two model nickel corphinoids investigated, which have all of the structural features of the natural chromophore, were synthesized by A. Fässler, A. Pfaltz, and A. Eschenmoser (*J. Chem. Soc., Chem. Commun.* **1984**, 1365). Raman lines analogous to the core-size marker lines of metalloporphyrins are identified for the Ni corphinoids, and, just as for the Ni porphyrins, the frequencies for the group of Raman marker lines characterize the 4-, 5-, and 6-coordinate complexes. Further, complexes with two strong nitrogenous bases (e.g., piperidine) can be distinguished from complexes with weak basic ligands (e.g., methanol) on the basis of the frequencies of these Raman lines. Finally, Raman spectra of polycrystalline samples of the Ni corphinoid and its monoisothiocyanate complex show that the structures existing in solution differ markedly from the structures in the crystalline state. The Raman markers will be useful in elucidating the structure of coenzyme F₄₃₀ and its interaction with the nearby protein environment in component C of the methyl-S-coenzyme-M reductase system.

Methylreductase catalyzes the final step in the production of methane from carbon dioxide and hydrogen in methanogenic bacteria.^{1,2} Carbon dioxide may be replaced as a substrate in methanogenesis by other small molecules such as methanol, formate, and acetate.² The final step in methanogenesis is the two-electron reduction of the methyl group of the intermediate methyl-S-coenzyme M (2-(methylthio)ethanesulfonate)¹ to methane. Methyl-coenzyme M methylreductase from *Methanobacterium thermoautotrophicum* has been purified to homogeneity³⁻⁵ and shown to contain cofactor F₄₃₀, a nickel-containing tetrapyrrole derivative.⁶⁻⁸ Recently, the structure **1** of factor F₄₃₀



was determined.⁹⁻¹¹ F₄₃₀ is a nickel corphinoid derivative that has all four pyrrole rings reduced. The corphinoid macrocycle incorporates aspects of both the corrins and the porphyrins in that the molecule has the carbon-nitrogen skeleton of the porphyrin and the conjugation system found in corrins.¹² Peripheral substitution

of the uroporphinoid macrocycle of F₄₃₀ includes two fused rings, one of which connects a β carbon of pyrrole D to the adjacent bridging carbon between pyrroles C and D.

It is important to elucidate the role of F₄₃₀ in the production of methane because biomimetic chemical or photochemical production of methane is a process that has commercial utility as a source of fuels and chemical feedstocks. The mechanism of action of the methylreductase enzyme is also of interest in the area of catalytic C-H bond activation chemistry. Speculation concerning the catalytic function of F₄₃₀ has centered on its pronounced affinity for axial ligands, ruffling of the tetrapyrrole ligand, and the ability of Ni(II) in F₄₃₀ to reversibly reduce to Ni(I).⁹⁻¹⁵

Here, the identification of several structure-sensitive resonance Raman lines that characterize the 4-, 5-, and 6-coordinate com-

- (1) Taylor, C. D.; Wolfe, R. S. *J. Biol. Chem.* **1974**, *249*, 4879.
- (2) Gunsalus, R. P.; Wolfe, R. S. *Biochem. Biophys. Res. Commun.* **1977**, *76*, 790.
- (3) Ellefson, W. L.; Wolfe, R. S. *J. Biol. Chem.* **1981**, *256*, 4259.
- (4) Ellefson, W. L.; Whitman, W. B.; Wolfe, R. S. *Proc. Natl. Acad. Sci. U.S.A.* **1982**, *79*, 3707.
- (5) Noll, K. M.; Rinehart, K. L., Jr.; Tanner, R. S.; Wolfe, R. S. *Proc. Natl. Acad. Sci. U.S.A.* **1986**, *83*, 4238.
- (6) Gunsalus, R. P.; Wolfe, R. S. *FEMS Microbiol. Lett.* **1978**, *3*, 191.
- (7) Diekert, G.; Klee, B.; Thauer, R. K. *Arch. Microbiol.* **1980**, *124*, 103.
- (8) Whitman, W. B.; Wolfe, R. S. *Biochem. Biophys. Res. Commun.* **1980**, *92*, 1196.
- (9) Pfaltz, A.; Juan, B.; Fässler, A.; Eschenmoser, A.; Jaenchen, R.; Gilles, H. H.; Diekert, G.; Thauer, R. K. *Helv. Chim. Acta* **1982**, *65*, 828.
- (10) Livingston, D. A.; Pfaltz, A.; Schreiber, J.; Eschenmoser, A.; Ankel-Fuchs, D.; Möll, J.; Jaenchen, R.; Thauer, R. K. *Helv. Chim. Acta* **1984**, *67*, 334.
- (11) Hausinger, R. P.; Orme-Johnson, W. H.; Walsh, C. *Biochemistry* **1984**, *23*, 801.
- (12) Johnson, A. P.; Wehrli, P.; Fletcher, R.; Eschenmoser, A. *Angew. Chem., Int. Ed. Engl.* **1968**, *7*, 623.
- (13) Fässler, A.; Pfaltz, A.; Kräutler, B.; Eschenmoser, A. *J. Chem. Soc., Chem. Commun.* **1984**, 1365.
- (14) Krafky, C.; Fässler, A.; Pfaltz, A.; Kräutler, B.; Juan, B.; Eschenmoser, A. *J. Chem. Soc., Chem. Commun.* **1984**, 1368.
- (15) Jaun, B.; Pfaltz, A. *J. Chem. Soc., Chem. Commun.* **1986**, 1327.

[†] This work performed at Sandia National Laboratories, supported by the U.S. Department of Energy, Contract DE-AC04-76DP00789, and the Gas Research Institute, Contract 5082-260-0767.

Table I. Raman Line Frequencies for F₄₃₀ and Model Nickel Corphinoid Complexes (and Shifts Relative to the Four-Coordinate Nickel Corphinoid in Methylene Chloride)^a

2 CH ₂ Cl ₂	2 powder	2(NCS) CH ₂ Cl ₂	2(NCS) powder	2 MeOH	2 piperidine	F ₄₃₀ ^b H ₂ O
1317	sh ^c	sh	sh			
1347	1334 (-13)	1337 (-10.6)	1334 (-13)	1335 (-12.2)	1333 (-14.4)	~1310
1376	1364 (-12)	1366 (-9.9)	~1365	~1366	~1366	
1384	1378 (-6)	1375 (-8.8)	1373 (-11)	1376 (-8.8)	1375 (-9.4)	1384
1402	1398 (-4)	1394 (-8.2)	1392 (-10)	1395 (-6.6)	1393 (-9.0)	
1502	~1485	1488	1485 (-17)	solvd	1485	
1548	1559 (11)	1551 (3.0)	1559 (11)	1558 (9.8)	1555 (7.4)	1530, 1562
1586	1615 (29)	1588 (1.8)	1592 (6)	1595 (8.8)	1595 (8.6)	
1641	1632 (-9)	1631 (-10.0)	1625 (-16)	1628 (-13.0)	1625 (-16.4)	1628

^a Shifts obtained from Raman difference spectra are given to 0.3-cm⁻¹ accuracy for most lines; see text. ^b Taken from ref 19. ^c sh = shoulder. ^d solvd = obscured by solvent line.

plexes of a nickel corphinoid **2** is reported. The F₄₃₀ model **2** has all of the structural features characteristic of coenzyme F₄₃₀.^{13,14} Although the nature of the peripheral substituents differs from F₄₃₀, the model Ni corphinoid has substituents at all macrocycle positions characteristic of F₄₃₀ and, thus, the model has the same π -conjugation system as the biological chromophore. The major difference in the model corphinoid **2** and F₄₃₀ **1** is the nitrile substituents at the meso position between rings C and D and at an α carbon of ring B. The nitrile substituents provide analogues of the fused ring attachments at these positions in F₄₃₀. The Ni corphinoid is 4-coordinate in methylene chloride, but 6-coordinate complexes are obtained in neat methanol or piperidine. In the latter coordinating solvents, solvent molecules are added axially at the Ni(II) ion above and below the macrocycle plane. The 5-coordinate complex investigated is the monoisothiocyanate (NCS⁻) complex of **2** in CH₂Cl₂.^{13,14} The Raman lines in the 1280–1680-cm⁻¹ region vary with the state of axial ligation in a manner similar to the core-size marker lines^{16,17} of the corresponding Ni porphyrins.

On the basis of the frequencies of the marker lines, a comparison of the Ni corphinoids in the form of a polycrystalline powder and in solution can be made. The 5-coordinate isothiocyanate complex is known to form 6-coordinate dimers in the crystal.¹⁴ Thus, it is not surprising to find that the crystal Raman spectrum of the NCS complex is closer to the 6-coordinate complexes obtained in coordinating solvents than to the 5-coordinate complex in CH₂Cl₂. The Raman data also show large differences in the structure of the 4-coordinate species when in the crystal and in methylene chloride solution.

Materials and Methods

The Ni corphinoid **2** and the monoisothiocyanate complex were prepared as described previously.¹³ They were kindly provided by A. Eschenmoser, A. Pfaltz, and A. Fässler of the Eidgenössische Technische Hochschule in Zürich. Solutions of the corphinoid for Raman and absorption spectra were prepared by dissolving the Ni corphinoid or the Ni-corphinoid-NCS complex in the appropriate neat solvent (CH₂Cl₂, piperidine, methanol). The concentration of the chromophore was 1–3 × 10⁻⁴ M. At concentrations below 10⁻³ M the chromophores are monomeric.¹⁴

The Raman spectra were obtained on a Raman difference spectrometer described previously.¹⁸ Briefly, the Raman spectra of pairs of solution samples were obtained simultaneously so that the frequency comparisons are accurate to ±0.3 cm⁻¹ for the strong Raman lines and to about ±0.5 cm⁻¹ for the weak but well-resolved lines.

For the spectra, the aerobic solution samples were rotated at 100 Hz to prevent heating. The sample temperature under these conditions is room temperature (21–23 °C). Laser power in the 413.1-nm line of the Kr⁺ laser was always less than 300 mW and typically about 70 mW. For the stationary polycrystalline powders the laser power was <<5 mW. The 90° scattering geometry was used in all cases. Sample decomposition was not observed either in successive scans of the Raman spectrum during signal averaging (typically five 30-min scans) or in the absorption spectra taken before and after laser irradiation.

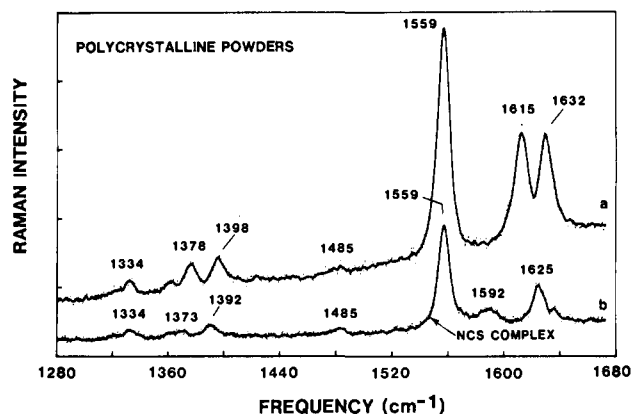


Figure 1. Resonance Raman spectra of the F₄₃₀ model nickel corphinoid (a) and the monoisothiocyanate nickel corphinoid complex (b) in the form of polycrystalline powders.

Results

The Ni corphinoid **2** is a yellow nonfluorescent compound with an absorption maximum at 412 nm in methylene chloride.¹³ The bis(methanol)-Ni corphinoid complex has a slightly red-shifted absorption band at 417 nm. The absorption maximum of the 5-coordinate NCS complex is red shifted to 419 nm and the bis(piperidine) complex has its absorption maximum even further to the red at 437 nm. The intensity of the transition indicates a $\pi \rightarrow \pi^*$ transition of the conjugated system of the macrocycle.

The Raman spectra were obtained with 413.1-nm laser radiation which is near resonance with the $\pi \rightarrow \pi^*$ band of all the Ni corphinoid complexes. Typical resonance Raman spectra in the 1280–1680-cm⁻¹ region are shown in Figures 1 and 2 and the vibrational frequencies are listed in Table I. Frequency differences are given relative to the 4-coordinate Ni corphinoid in CH₂Cl₂. In Figure 1 the Raman spectra of the solid samples are presented. Spectrum a is from **2** and spectrum b is from the NCS complex of **2**. The spectra are somewhat similar, but notable differences in frequency are observed for the two highest frequency Raman lines. In addition, small but significant (~5 cm⁻¹) frequency differences are detected in the 1378- and 1398-cm⁻¹ lines (see Table I).

The Raman spectra shown in Figure 1 can be compared with the CH₂Cl₂ solution spectra of the Ni corphinoid and its NCS complex given in Figure 2, a and b, respectively. Comparison of the 4-coordinate species existing in noncoordinating solvent with the polycrystalline sample of this compound shows that the spectra are grossly different. Shifts as large as 29 cm⁻¹ occur upon crystallization. The large shifts indicate a markedly different molecular structure of the Ni corphinoid in solution and in the polycrystalline powder. Axial coordination of nickel with nitrile substituents on neighboring corphinoids might be anticipated for the polycrystalline powder (vide infra). Indeed, axial coordination may occur since the solid-phase Raman spectrum bears some similarity to the spectra of the axially coordinated species as can be seen from Table I. However, based on the unique spectrum of the polycrystalline Ni corphinoid, the structure in the crystal must be quite different from that of the other axially coordinated

(16) Spaulding, L. D.; Chang, C. C.; Yu, N.-T.; Felton, R. H. *J. Am. Chem. Soc.* **1975**, *97*, 2517.

(17) Spiro, T. G. In *Iron Porphyrins Part II*; Lever, A. B. P., Gray, H. B., Eds.; Addison-Wesley: Reading, MA, 1982; p 89.

(18) Shelnutt, J. A. *J. Phys. Chem.* **1983**, *87*, 605.

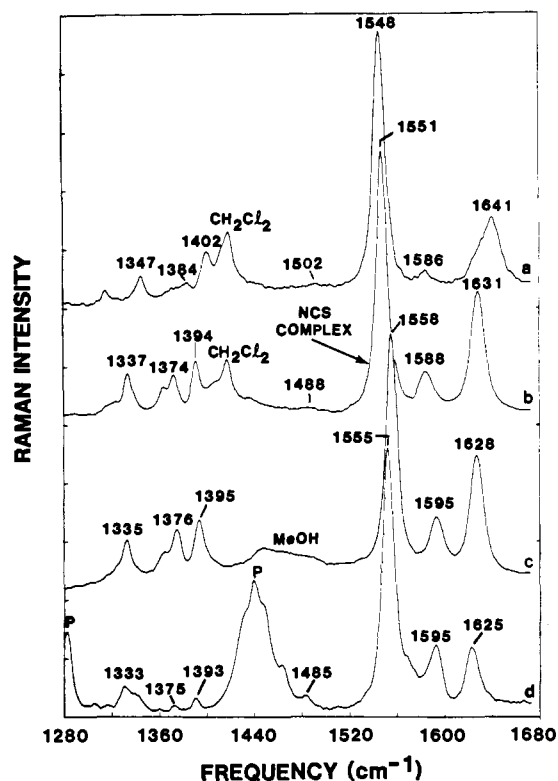


Figure 2. Resonance Raman spectra of the nickel corphinoid in CH_2Cl_2 (a), the monoisothiocyanate complex in CH_2Cl_2 (b), the bis(methanol) complex in methanol (c), and the bis(piperidine) complex in neat piperidine (d). Solvent lines are indicated (P = piperidine).

species that we have investigated.

The crystal structure of the monoisothiocyanate complex is known and shows that a novel dimer occurs in the crystal.¹⁴ The NCS ligand occupies one axial position of each Ni corphinoid unit of the dimer, and the nitrile substituent of pyrrole B of the adjacent molecule of the dimer provides the second axial ligand giving a 6-coordinate complex in the solid. Therefore, it is not surprising to find that the crystalline NCS complex has a spectrum closer to the spectra of the solution, 6-coordinate complexes (especially, the bis(piperidine) complex) than to the solution 5-coordinate complex; see Table I.

For the solution spectra in Figure 2 we observe the largest differences in frequencies when comparing the spectra of the axially coordinated species which is paramagnetic to the 4-coordinate diamagnetic Ni corphinoids.¹⁴ Small frequency differences are noted between the 5-coordinate complex and the weak- and strong-field 6-coordinate complexes uniquely identifying each of these axially coordinated species. Clearly, the large effect on the Raman spectrum results from the change in the interaction of the nickel ion with the macrocycle brought about by the change in d-orbital occupation. Nevertheless, changes in the electronic structure are evident in the large absorption spectral changes that accompany the change from weak- to strong-field ligands. These latter electronic changes result in only small changes in the high-frequency vibrations. Weak coupling between vibrational and electronic motion is to be expected for a π -delocalized macrocycle, so that large electronic structure changes may be evident in the absorption spectrum but the changes may only weakly influence the vibrational frequencies. Also, the Raman spectrum reflects only the ground-state properties, whereas the absorption spectrum can be affected by excited-state differences as well.

Discussion

The general features of the reported¹⁹ resonance Raman spectrum of F_{430} and the spectra of the related Ni corphinoid

complexes (see Table I) show striking similarities. However, the reported spectrum is actually that of a mixture of the salt-extracted and cytosol-free forms of F_{430} ,²⁰ therefore, it is not yet possible to determine the exact correspondence between the vibrations of F_{430} and the model corphinoid. Nevertheless, on the basis of the similarities we can expect our results for the model Ni corphinoid, generally, to carry over to the biological chromophore. The Ni corphinoid spectra also bear some resemblance to the Ni porphyrin²¹ and Ni chlorin^{22,23} Raman spectra. In particular, the Ni corphinoid spectra display a larger number of Raman-active modes than the Ni porphyrins as a result of the low symmetry of the corphinoids. A similar increase in the number of Raman-active modes, especially in the 1300–1400- cm^{-1} region, is noted for metallochlorins,^{22,23} which also have low symmetry. A comparison of the general features of the Ni corphinoid and Ni porphyrin Raman spectra is informative.

Metalloporphyrin Core-Size Marker Lines^{16,17,24,25} and Axial Ligation. For pyrrole-substituted metalloporphyrins, a group of high-frequency (1280–1680- cm^{-1}) lines, including ν_3 , ν_2 , ν_{19} , and ν_{10} , are known to inversely correlate with the center-to-nitrogen_{pyrrole} distance or core size for a wide variety of metals and porphyrin ligands.^{16,17} The same is true for the meso-substituted metalloporphyrins,^{17,24,25} and, for these porphyrins, the oxidation-state marker line ν_4 ^{26,27} also becomes more core-size sensitive.²⁵ Roughly, a decrease in frequency of 1 cm^{-1} in a core-size line represents an increase in core size of $\sim 0.002 \text{ \AA}$.¹⁷ Although a correlation with core size has not been explicitly shown for reduced porphyrins, for the metallochlorins the Raman lines in this region of the spectrum appear to behave in a fashion similar to that observed for the metalloporphyrins.^{22,23}

For the Ni porphyrins, in particular, the relationship between core size and Raman frequencies has been verified and documents axial ligation-induced core expansion.^{21,28–30} The 0.08- Å expansion of the core that occurs upon axial ligation in the crystal^{31,32} is well predicted based on the changes in marker line frequencies that accompany addition of two axial ligands in solution studies. For example, a decrease of 41 cm^{-1} occurs for ν_{10} upon axial ligation of two strong field ligands (pyrrolidine) to nickel protoporphyrin IX (Ni(ProtoP)). The decrease predicts the observed expansion of 0.08 Å (based on 0.0019 $\text{Å}/\text{cm}^{-1}$ for ν_{10}). The meso-substituted Ni porphyrins show similar core expansion upon axial ligation. In particular, nickel tetramethylpyridinium porphyrin (Ni(TMePyP)) has 4-coordinate ν_3 at 1475 cm^{-1} (MeOH) and 6-coordinate ν_3 at 1446 cm^{-1} (imidazole).³³ For the meso-substituted porphyrins, the dependence of ν_3 on frequency is 0.0024 $\text{Å}/\text{cm}^{-1}$; thus, the 29- cm^{-1} decrease in frequency represents a core expansion of 0.07 Å .

To summarize, axial ligation in the Ni porphyrins induces a

(20) Hartzell, P. L.; Wolfe, R. S. *Proc. Natl. Acad. Sci. U.S.A.* **1986**, *83*, 6726.

(21) Shelnutz, J. A.; Alston, K.; Ho, J.-H.; Yu, N.-T.; Yamamoto, T.; Rifkind, J. M. *Biochemistry* **1986**, *25*, 620.

(22) Andersson, L. A.; Loehr, T. M.; Chang, C. K.; Mauk, A. G. *J. Am. Chem. Soc.* **1985**, *107*, 182.

(23) Andersson, L. A.; Loehr, T. M.; Sotiriou, C.; Wu, W.; Chang, C. K. *J. Am. Chem. Soc.* **1986**, *108*, 2908.

(24) Stong, J. D.; Spiro, T. G.; Kubaska, R. J.; Shupack, S. I. *J. Raman Spectrosc.* **1980**, *9*, 312.

(25) Chottard, G.; Battioni, P.; Battioni, J.-P.; Lange, M.; Mansuy, D. *Inorg. Chem.* **1981**, *20*, 1718.

(26) Yamamoto, T.; Palmer, G.; Gill, D.; Salmeen, I. T.; Rimai, L. *J. Biol. Chem.* **1973**, *248*, 5211.

(27) Spiro, T. G.; Streckas, T. C. *J. Am. Chem. Soc.* **1974**, *96*, 338.

(28) Shelnutz, J. A.; Alston, K.; Findsen, E. W.; Ondrias, M. R.; Rifkind, J. M. In *Porphyrins: Excited States and Dynamics*; Gouterman, M., Rentzepis, P. M., Straub, K. D., Eds.; American Chemical Society: Washington, DC, 1986; chapter 16.

(29) Findsen, E. W.; Alston, K.; Shelnutz, J. A.; Ondrias, M. R. *J. Am. Chem. Soc.* **1986**, *108*, 4009.

(30) Findsen, E. W.; Shelnutz, J. A.; Friedman, J. M.; Ondrias, M. R. *Chem. Phys. Lett.* **1986**, *126*, 465.

(31) Cullen, D. L.; Meyer, E. F., Jr. *J. Am. Chem. Soc.* **1974**, *96*, 2095.

(32) Kirner, J. F.; Garofalo, J., Jr.; Scheidt, W. R. *Inorg. Nucl. Chem. Lett.* **1975**, *11*, 107.

(33) Shelnutz, J. A.; Shelnutz, J. J.; Findsen, E. W.; Ondrias, M. R., to be submitted for publication.

(19) Schiemke, A. K.; Eirich, L. D.; Loehr, T. M. *Biochim. Biophys. Acta* **1983**, *748*, 143.

decrease in frequency of a group of macrocycle vibrations. The decrease in frequency is a result of the core expansion caused by axial ligation. Axial ligation causes the core to expand primarily because of an induced d-d transition^{28-30,33-37} and to a lesser extent because of other electronic changes in the metal's interaction with the macrocycle³⁸⁻⁴⁰ (vide infra). The combined effect is that the frequencies of the Raman marker lines depend on whether zero, one, or two ligands are bound and on the field strength of the ligands. In fact, the frequency for each line of the group decreases in the order: 4-coordinate > 5-coordinate > 6-coordinate, weak field > 6-coordinate, strong field. As an example, for Ni(ProtoP) the frequencies of ν_4 (not a core-size marker line for Ni(ProtoP)) are 1377 (4-coordinate) > 1368 (5-coordinate) > 1365 cm^{-1} (6-coordinate, strong field); for the core-size marker ν_{10} they are 1658 (4-coordinate) > 1619 (5-coordinate) > 1616 cm^{-1} (6-coordinate, strong field). For some lines the differences between the 5- and 6-coordinate frequencies are large. An example is ν_3 for which 1519 (4-coordinate) > 1487 (5-coordinate) > 1476 cm^{-1} (6-coordinate, strong field).²¹

Nickel protoporphyrin binds only strong-field ligands, but Ni(TMePyP), in contrast, exhibits a much higher affinity for ligands adding both strong- and weak-field ligands. For Ni(TMePyP) the frequencies for ν_4 are 1375 (4-coordinate) > 1353 (6-coordinate, weak field) > 1347 cm^{-1} (6-coordinate, strong field); for ν_3 they are 1476 (4-coordinate) > 1452 (6-coordinate, weak field) > 1447 cm^{-1} (6-coordinate, strong field).³³

For the nickel porphyrins more than half of the decrease in marker line frequencies (core size) that occurs upon formation of the 6-coordinate complex results directly from the change in spin state from $S = 0$ to $S = 1$. Upon absorption of light by a $\pi \rightarrow \pi^*$ transition of the 4-coordinate diamagnetic ($S = 0$) species, the excited Ni porphyrin decays rapidly (<20 ps) to a long-lived (>250 ps) d-d state ($S = 1$).³⁴⁻³⁶ Molecular orbital calculations³⁷ show that the net photoinduced d-d transition moves one electron from the filled d_{z^2} orbital of the 4-coordinate species to the antibonding $d_{x^2-y^2}$ orbital that is directed toward the pyrrole nitrogens. In this way the metal's interaction with the ring is destabilized and core expansion results. The frequencies of the core-size marker lines for this transient 4-coordinate ($S = 1$) state are found to be intermediate between the 4- and 5-coordinate values.^{29,30} For example, ν_{10} of the transient species is found at 1629 cm^{-1} for Ni(ProtoP).³⁰

The d-d transition is also induced by addition of ligands which raises the energy of the d_{z^2} orbital. Moreover, binding of ligands further reduces the marker line frequencies slightly. Thus, the order of the marker line frequencies for all species is 4-coordinate ($S = 0$) > 4-coordinate ($S = 1$) > 5-coordinate ($S = 1$) > 6-coordinate ($S = 1$), weak > 6-coordinate ($S = 1$), strong.

Nickel Corphinoid Structure-Sensitive Raman Lines. The nickel corphinoid complexes might be expected to exhibit Raman lines that behave in a manner analogous to the porphyrin core-size marker lines. One reason is that the corphinoids have the same molecular structure as the porphyrins in that the methine bridges are all present. This is important because the core-size sensitivity is thought to result from $C_{\text{methine}}-C_{\alpha}$ stretching contributions to these modes.^{17,41,42} Second, even though the π -conjugation system of the corphinoids is not as extensive as for the porphyrins, the conjugation system does include the methine bridges, and, consequently, the modes corresponding to the marker lines should still be resonantly enhanced for the corphinoids.

Indeed, the Ni corphinoid has lines in the 1280-1680- cm^{-1} region of the Raman spectrum that behave upon axial ligation

like the core-size markers. In particular, the line at 1347 cm^{-1} of the 4-coordinate species decreases to 1337 cm^{-1} for the 5-coordinate complex, decreases further to 1335 cm^{-1} for the weak-field 6-coordinate complex, and decreases further yet to 1333 cm^{-1} for the strong-field 6-coordinate complex. Similarly, the line at 1641 cm^{-1} of the 4-coordinate species decreases in the order: 4-coordinate > 5-coordinate > 6-coordinate, weak > 6-coordinate, strong (see Table I). Also just as for the Ni porphyrins, the largest part of the shift in frequency comes with the addition of the first ligand (and the d-d transition). Small additional decreases in frequency accompany binding of a second ligand or an increase in the ligand's basicity. It is also significant that the direction of the shifts in the Ni corphinoid 1347- and 1641- cm^{-1} vibrations is the same as is observed for the porphyrin core-size marker lines. The magnitudes of the axial ligand induced shifts ($\sim 15 \text{ cm}^{-1}$) are somewhat smaller than for the porphyrins. It should be noted also that the two lines at 1548 and 1586 cm^{-1} increase in frequency for the 4-, 5-, and 6-coordinate species.

Further, if we take the 1347- and 1641- cm^{-1} lines to be core-size marker lines for corphinoids as well as for porphyrins, then we can draw other conclusions about the structure. First, as for the Ni porphyrins, axial ligation results in expansion of the corphinoid core and the Raman lines provide a way of measuring the relative expansion under various circumstances. For example, we now see that two strong-field ligands cause the corphinoid core to expand more than two weak-field ligands or a single ligand.

Crystal and Solution Structures of Ni Corphinoids. Probably the most valuable finding of the present investigation is that the corphinoid Raman lines provide a method of distinguishing the coordination number and field strength of the axial ligand(s). The result suggests that Raman spectroscopy will be a useful probe of the local environment of F_{430} in its protein-bound form. The structure-sensitive Raman lines also allow a comparison of Ni corphinoid structures in solution and in the polycrystalline powder. The comparison of Raman spectra of the polycrystalline and solution samples confirms that the monoisothiocyanate Ni corphinoid complex is actually 6-coordinate in the solid as already known from the X-ray crystal structure.¹⁴ The Raman spectrum of the NCS complex in the solid is a bit closer to the spectrum of the bis(piperidine) complex than the methanol complex, which suggests that isothiocyanate and nitrile ligands act as strong-field ligands.

On the other hand, the Raman data for the 4-coordinate Ni corphinoid when in the crystal is not at all similar to the 4-coordinate species in solution. One possibility is that in the solid a 5-coordinate complex may result from axial coordination of a nitrile substituent of a nearby Ni corphinoid in the crystal. However, the fact that the crystal spectrum is markedly different from that of the solution 5-coordinate complex argues against this hypothesis.

Macrocycle Ruffling in Nickel Corphinoids and Porphyrins. Another explanation of the differences in the crystal and solution, 4-coordinate Ni corphinoid spectra is based on ruffling of the corphinoid ring and is made in analogy with the differences in crystal and solution Raman spectra of nickel octaethylporphyrin (Ni(OEP)).^{31,32} Ni(OEP) exists in both a square-planar (D_{4h}) configuration in the triclinic form and a ruffled (D_{2d}) configuration in the tetragonal form. The core-size marker lines of the two crystalline forms differ in frequency by as much as 20 cm^{-1} .¹⁶ The spectrum of the square-planar form is much closer to the spectrum of Ni(OEP) in solution where the molecule is expected to take on a square-planar geometry. It should also be mentioned that the tetragonal ruffled form does not fall on the correlation between Raman frequency and core size. The core size is slightly smaller (0.03 Å) for the ruffled porphyrin even though the large decrease in marker-line frequencies would predict the ruffled porphyrin to have a larger core than the planar form. It is known that the core-size marker lines depend on structural parameters other than core size for metalloporphyrins that depart from a near-planar conformation.¹⁷

For the Ni corphinoid also, ruffling may account for the frequency differences between the crystal and solution Raman

(34) Kim, D.; Kirmaier, C.; Holten, D. *Chem. Phys.* **1983**, *75*, 305.

(35) Kim, D.; Holten, D. *Chem. Phys. Lett.* **1983**, *98*, 584.

(36) Holten, D.; Gouterman, M. Proceedings of the Symposium on Optical Properties and Structure of Tetrapyrroles, Konstanz, Aug 12-17, 1984.

(37) Ake, R. L.; Gouterman, M. *Theor. Chim. Acta* **1970**, *17*, 408.

(38) Shelnutt, J. A.; Ondrias, M. R. *Inorg. Chem.* **1984**, *23*, 1175.

(39) Shelnutt, J. A.; Straub, K. D.; Rentzepis, P. M.; Gouterman, M.; Davidson, E. R. *Biochemistry* **1984**, *23*, 3946.

(40) Shelnutt, J. A. *J. Am. Chem. Soc.* **1983**, *105*, 774.

(41) Kitagawa, T.; Abe, M.; Ogoshi, H. *J. Chem. Phys.* **1978**, *69*, 4516.

(42) Abe, M.; Kitagawa, T.; Kyogoku, Y. *J. Chem. Phys.* **1978**, *69*, 4526.

spectra. Four-coordinate Ni corphinoids are known to crystallize in a highly ruffled conformation as illustrated by the nickel octaethyl pyrrocorphinato structure.^{14,43} Thus, in analogy with the Ni(OEP) case, the Raman spectrum of the crystal is that of a ruffled corphinoid, while the solution spectrum is that of a more planar Ni corphinoid. The core size is expected to be smaller for the ruffled structure than for the planar one. Hence, core contraction occurs and the large decrease in Ni corphinoid marker line frequencies for the crystalline form (1347 \rightarrow 1334 cm^{-1} and 1641 \rightarrow 1632 cm^{-1}) likely results from ruffling of the macrocycle and not from expansion of the core.

Recently, Waditschatka et al., using proton NMR spectroscopy, showed that Ni *cccc*-octaethyl-pyrrocorphinato exchanges between two enantiomorphically ruffled conformers.⁴⁴⁻⁴⁶ The exchange rate was found to be $2.9 \times 10^4 \text{ s}^{-1}$ at 25 °C. If in the present case exchange between two distinguishable ruffled forms is occurring, inversion of the ruffled forms of the Ni corphinoid must occur on a subnanosecond time scale because the faster Raman measurement shows no clear evidence of the presence of two forms—at least not forms similar to the crystalline form, which we believe takes on a ruffled structure. Another possibility, however, is that any ruffled forms existing in solution have nearly identical Raman spectra that are distinct from the ruffled species occurring in the polycrystalline solid.

Very recently we have completed an extensive Raman investigation of free and salt-extracted forms of F_{430} and of methyl-

reductase.^{47,48} Ruffling appears to play a role in the spectra of F_{430} in aqueous solution as the spectrum of the ruffled, 4-coordinate form is different from that of the 4-coordinate model, this in spite of the fact that the 6-coordinate forms of F_{430} and the model **2** are almost identical. Model **2** is sterically hindered at the periphery in a manner different from the two isomers of F_{430} and appears not to ruffle as easily as either the pyrrocorphinato or free F_{430} .

Conclusions

It has been shown that excellent quality resonance Raman spectra of Ni corphinoids, related to cofactor F_{430} of the methylreductase system, can be obtained. In fact, the Raman spectra of the Ni corphinoid complexes are strikingly similar to the reported spectrum of F_{430} . The high-frequency Raman lines of the Ni corphinoid vary in a manner analogous to the core-size marker lines of metalloporphyrins. In particular, the analogous structural marker lines identified for the Ni corphinoid provide a means by which the number and type of axial ligand(s) can be determined. The Ni corphinoid Raman lines, therefore, provide a useful structural probe of Ni corphinoids such as F_{430} in various environments including a site in a protein.^{47,48}

Acknowledgment. I thank A. Eschenmoser, A. Pfaltz, and A. Fässler for providing the Ni corphinoids for the Raman studies and A. Eschenmoser for a useful communication on the interpretation of the data. I also thank A. K. Shiemke, R. A. Scott, and L. A. Andersson for helpful discussions.

(43) Waditschatka, R.; Kratky, C.; Juan, B.; Heinzer, J.; Eschenmoser, A. *Angew. Chem.*, to be published.

(44) Waditschatka, R.; Kratky, C.; Juan, B.; Heinzer, J.; Eschenmoser, A. *J. Chem. Soc., Chem. Commun.* **1985**, 1604.

(45) Kratky, C.; Waditschatka, R.; Angst, C.; Johansen, J. E.; Plauevent, J. C.; Schreiber, J.; Eschenmoser, A. *Helv. Chim. Acta* **1985**, *68*, 1312.

(46) Eschenmoser, A. *Ann. N. Y. Acad. Sci.* **1986**, *471*, 108.

(47) Shiemke, A. K.; Scott, R. A.; Shelnut, J. A. *J. Am. Chem. Soc.*, submitted.

(48) Shelnut, J. A.; Shiemke, A. K.; Scott, R. A., ACS Division of Fuel Chem. Preprints, Aug. 31-Sept. 4, 1987, in press.

Temperature and Solvent Dependence of Scalar Coupling Constants in Salts of $trans\text{-HFe}(\text{CO})_3\text{PR}_3^-$

Carlton E. Ash, Marcetta Y. Darensbourg,* and Michael B. Hall

Contribution from the Department of Chemistry, Texas A&M University, College Station, Texas 77843. Received November 28, 1986

Abstract: Salts of $[trans\text{-HFe}(\text{CO})_3\text{PR}_3]^-$ ($\text{PR}_3 = \nu(\text{OMe})_3, \text{P}(\text{OEt})_3, \text{PPh}_3, \text{and P}(\text{Et})_3$) are observed to give variable NMR parameters depending on temperature and solvent. Of all the NMR parameters, the changes in phosphorus to hydride coupling constants are most dramatic. For example, $[\text{bis}(\text{triphenylphosphine})\text{iminium}^+][\text{HFe}(\text{CO})_3\text{P}(\text{OEt})_3]^-$ showed a 20-Hz change and sign inversion in J_{PH} in tetrahydrofuran over a temperature range of +50 to -70 °C. Both variable-temperature infrared spectroscopy and molecular orbital calculations have been conducted to explore the cause of such extraordinary behavior. The infrared data best fit a mechanism of changing H-Fe-CO angle enforced by a solvent stabilization of an internal dipole moment in the anion. Unlike the above compounds, anionic metal hydrides with phosphorus donor ligands positioned *cis* to the hydride ligand showed little dependence of temperature and solvent on scalar coupling constants.

The preparation and reactivity of salts of $trans\text{-HFe}(\text{CO})_3\text{PR}_3^-$ ($\text{PR}_3 = \text{PMe}_3, \text{PEt}_3, \text{PPh}_2\text{Me}, \text{PPh}_3, \text{P}(\text{OEt})_3, \text{P}(\text{OMe})_3$) have recently been reported.¹ An X-ray crystal structure determination of a typical hydride, $[\text{Et}_4\text{N}^+][\text{HFe}(\text{CO})_3\text{PPh}_3]^-$ (**1**), showed the anion to be of pseudo-trigonal-bipyramidal (TBP) geometry (C_{3v} symmetry) with the three CO ligands bent out of the equatorial plane and toward the (unlocated) hydride ligand by 9.5 (3)°. The $\nu(\text{CO})$ IR spectral data for **1** and analogous hydrides listed above

were, in both solution and in the solid state, consistent with the molecular structure observed for **1**, i.e., of *trans* geometry. In only one derivative has a different geometrical isomer been observed: the hydride of $\text{PPN}^+ cis\text{-HFe}(\text{CO})_3\text{P}(\text{OPh})_3^-$ (**2**) is axial and the $\text{P}(\text{OPh})_3$ ligand is equatorial in a pseudo-TBP structure.²

The signal for the hydride resonance for all hydride derivatives was about -9 (± 0.5) ppm upfield from tetramethylsilane, and showed only a small dependence on P-donor ligand, solvent,

(1) Ash, C. E.; Delord, T.; Simmons, D.; Darensbourg, M. Y. *Organometallics* **1986**, *5*, 17.

(2) Ash, C. E.; Kim, C. M.; Darensbourg, M. Y.; Rheingold, A. *Inorg. Chem.* **1987**, *26*, 1357.